Bull. Chem. Soc. Jpn., 70, 2981—2986 (1997)

Rotator Phase in Dodecylammonium Chloride Studied by ^{1}H and ^{2}H Solid NMR and Thermal Measurements

Susumu Tanaka, Noriko Onoda-Yamamuro, Shin'ichi Ishimaru, and Ryuichi Ikeda*

Department of Chemistry, University of Tsukuba, Tsukuba 305

(Received July 14, 1997)

^{1}H NMR spin-lattice relaxation times, T_1 and $T_{1\rho}$, the second moment M_2 of ^{1}H NMR linewidth, ^{2}H NMR spectra, powder X-ray diffraction, electrical conductivity, and thermal measurements have been performed on $C_{12}H_{25}NH_3Cl$ and $C_{12}H_{25}ND_3Cl$ in the range between room temperature and the melting point. From these measurements, the presence of the rotator phase was revealed above ca. 345 K, where a highly disordered structure characterized by the rapid 2-D self-diffusion as well as the axial rotation of the cations taking place in the lamellar-type double layer structure is formed. These molecular motions, the crystal structure and the thermal nature found in this phase indicate that the rotator phase is close to the plastic crystal and can be described as "a low-dimensional plastic phase". The determined dynamic parameters of molecular motions in this phase were compared with those in the values reported in the rotator phases of short alkyl chain analogues.

"Rotator phase", first discovered in *n*-paraffins[1] in a narrow temperature range just below the melting point, has been recently shown to occur in alkylammonium chlorides[2—5] of C_3 to C_{10} in a wide temperature range over 200 K. This phase is characterized by the onset of axial rotation of all constituent molecules or ions about their long axis. In alkylammonium chlorides consisting of rod-like cations and spherical anions alternately packed in a tetragonal lattice (*P4/nmm*) of lamellar-type double layer structure,[6] we found a new characteristic molecular motion in the rotator phase, i.e., 2-D self diffusion of cations along the lamellar plane perpendicular to the cationic long axis.[3] Upon heating, the rotator phases with alkyl chain longer than C_5 have been reported to transform into a smectic liquid crystalline phase above the melting point, and another non-isotropic liquid phase was observed above the clearing point of this smectic phase.[7] The highly disordered structure of the rotator phase together with small melting entropies (ΔS_m)[7,8] close to or less than 20 J K^{-1} mol^{-1},[9] accompanied by transition entropies (ΔS_{tr}) at transitions to the rotator phase larger than ΔS_m, suggests that the rotator phase is a kind of mesophase very close to the plastic crystal. On the other hand, the lamellar-type structure consisting of axially disordered long alkylammonium ions is rather analogous to that of the smectic liquid crystal, although the centres of gravity of constituent molecules are regularly arranged in the rotator phase, whereas, in most cases, they are disordered in liquid crystal. Here, we note that a liquid crystalline phase named as "smectic-B" has been reported to be crystalline phase with the axial rotation of molecules along the long axis; this phase may belong to an analogous kind of category to the present rotator phase.[10]

From these features of the rotator phase, it seems reasonable to assume it as an intermediate state between the plastic crystal and the liquid crystal. In the limit of the short alkyl chain, we have shown that NH_4X[11] and CH_3NH_3X (X : Br and I)[12,13] form plastic phases in the high-temperature ranges just below the melting points. With increasing the carbon number in the alkyl group, the structure becomes asymmetric and the rotator phase is formed around room temperature in compounds with longer than C_3.

Our interest is to discover, with further increase of the C-number, how properties in the rotator phase change, and whether they become close to the liquid crystal or not. In the present study, we selected dodecylammonium chloride, as a long chain alkylammonium salt. Dynamic properties in its rotator and related low-temperature phases are investigated.

Experimental

Dodecylammonium chloride, $C_{12}H_{25}NH_3Cl$ (abbreviated to DACl), was prepared by neutralizing dodecylamine (Aldrich 98 %) dissolved in ethanol with hydrochloric acid diluted with ethanol by 1 : 4 and evaporating solvents. The crude crystals obtained were recrystallized three times from a mixed solvent of ethanol and water by slow evaporation of solvent in a desiccator under dry nitrogen gas flow.

A partially deuterated analogue $C_{12}H_{25}ND_3Cl$ (abbreviated to DACl-d_3), was prepared by successive crystallizations from D_2O (99.8 % deuterated).

Powder X-ray diffraction were measured with a Rigaku CN2 155D5 and a Philips X'Pert PW3040/00 diffractometer using Cu $K\alpha$ radiation.

Differential scanning calorimetry (DSC) was performed on DACl and DACl-d_3 with a DSC120 calorimeter from Seiko Inc. using samples of ca. 10 mg sealed in an aluminum cell over a temperature range 240–470 K.

^{1}H NMR spin-lattice relaxation times T_1 and $T_{1\rho}$ were measured with a Bruker SXP-100 spectrometer at a Larmor frequency of 40 MHz with a Chino SU10-2121LNN temperature controller. T_1 was determined by the saturation recovery method, while $T_{1\rho}$ was obtained by the spin-lock method[14] applying an r.f. magnetic field

of 0.4 mT. The second moment M_2 of ^{1}H NMR linewidth was evaluated from the decay curve of solid echo signals using the $\pi/2_x-\tau-\pi/2_y$ pulse sequence.[15] ^{2}H spectra in DACl-d_3 were measured using a Bruker MSL-300 spectrometer at a Larmor frequency of 46.073 MHz.

The electrical conductivity was measured at 1 kHz by the two-terminal method using a home-made apparatus in a temperature range of 300—440 K. The powdered sample was pressed into a disc 1 cm in diameter and ca. 1 mm thick; graphite electrodes (Acheson Electrodag 199) were employed.

Results and Discussion

Thermal Measurements. The obtained DSC results on DACl are in fair agreement with those reported by Tsau and Gilson.[8] The melting entropies observed on DACl and DACl-d_3 are smaller than 20 J K^{-1} mol^{-1}; this value is one of the conditions for the formation of the plastic crystal.[9] It indicates that a highly disordered structure is realized below the melting temperature (T_m), suggesting the formation of the rotator phase analogous to the result in shorter alkyl chain compounds.[2—5] The three successive transitions observed on DACl (DACl-d_3) at 320 (321), 333 (334), and 345 (345) K, are therefore, assignable to those to the rotator phase. The highest-temperature transition observed at 345 K can correspond to that observed at 347 K with a transition enthalpy (ΔH_{tr}=2.91 kJ mol^{-1}) reported as the conformation melting by Busico et al.[7]

Powder X-Ray Diffraction. We measured powder X-ray diffraction for DACl at 358±2 K in the highest-temperature phase, expected to be the rotator phase. The observed pattern showed characteristic diffractions from the layer structure and at the same time, weak but clear peaks from the in-plane structure indicating the regular arrangements of the centers of gravity of long alkylammonium ions in this phase. The observed data were well indexed with a tetragonal structure with the lattice parameters a=5.02±0.01, c=32.5±0.1 Å and Z=2. These results agree well with a=5.12 and c=32.0 Å measured by Busico et al.[7] at 400 K. From the systematic absence of the diffraction peaks ($hk0: h+k\neq 2n$) observed, the space group was uniquely determined to be *P4/nmm*. By comparing these lattice parameters with the values reported in the rotor phases of the short alkyl chain ammonium chlorides,[6] we can see that this phase is isomorphous with the rotator phase, in which both cations and anions locating on the crystallographic C_4-axis form a lamellar-type double layer structure, and the axial rotation of the cations about the long axis and two-dimensional self-diffusion of both ions along the lamellar plane were observed.[3,5]

Dynamics in the Low-Temperature Phase (LTP). Second Moment (M_2) of ^{1}H NMR. Temperature dependences of second moments (M_2) of ^{1}H NMR linewidth measured in DACl and DACl-d_3 in a range of 110—410 K are shown in Fig. 1. The observed M_2 of 27×10^{-2} mT^2 at ca. 150 K can be explained by the reorientation model of the terminal CH_3-group about the C–C bond, because this value is explainable by the theoretical M_2 of 21.9×10^{-2} mT^2 calculated in DACl-d_3 using the Van Vleck equation.[16]. The M_2 decrease observed upon heating to ca. 300 K implies the onset of a new motion of the alkyl chain. In the short alkyl chain salts such as $C_4H_9NH_3X$ (X: Br, 1), the 180° flip or analogous two-site jumps of the entire alkyl chain were found in the low-temperature phases.[17,18] We can also expect a similar motion in the present system. We will discuss this more in detail in the ^{1}H T_1 and ^{2}H NMR spectra analyses given below.

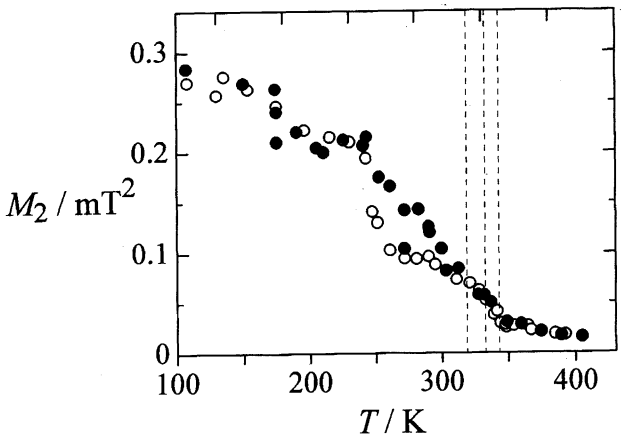

Fig. 1. Temperature dependences of second moment (M_2) of ^{1}H NMR linewidth observed in $C_{12}H_{25}NH_3Cl$ (DACl) (○) and $C_{12}H_{25}ND_3Cl$ (DACl-d_3) (●). Broken lines show the phase transition temperatures determined by DSC.

^{1}H NMR Spin-Lattice Relaxation Time (T_1). Temperature dependences of the ^{1}H NMR spin-lattice relaxation time (T_1) measured in DACl and DACl-d_3 are shown in Fig. 2. In LTP, each analogue gave T_1 minima, which can be attributed to a molecular motion and expressed by the BPP equation as[19]

$$T_1^{-1} = \frac{2}{3}\gamma^2 \Delta M_2 \left(\frac{\tau}{1+\omega^2\tau^2} + \frac{4\tau}{1+4\omega^2\tau^2} \right), \qquad (1)$$

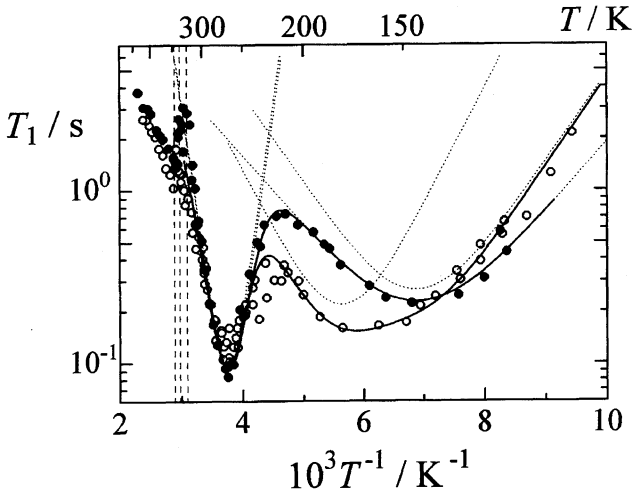

Fig. 2. Temperature dependences of ^{1}H NMR spin-lattice relaxation time T_1 observed in $C_{12}H_{25}NH_3Cl$ (DACl) (○) and $C_{12}H_{25}ND_3Cl$ (DACl-d_3) (●) at a Larmor frequency of 40 MHz. Solid lines are the best-fitted calculated values given in text. Dotted lines are contributions from respective molecular motions (see text). Broken lines show the phase transition temperatures determined by DSC.

where γ, ΔM_2, ω denote the proton gyromagnetic ratio, the reduction of M_2 by the motion, and the angular Larmor frequency, respectively. The observed T_1 curves plotted against T^{-1} are explainable by Eq. 1 using the Arrhenius relationship between τ and the motional activation energy (E_a) as given by

$$\tau = \tau_0 \exp\left(\frac{E_a}{RT}\right). \quad (2)$$

We observed two T_1 minima in LTP of DACl-d_3, which were fitted by two superimposed BPP minima given by Eqs. 1 and 2. The obtained best fit theoretical T_1 is shown in Fig. 2 and the determined values of motional parameters are listed in Table 1. By referring to the M_2 analysis given above, the broad minimum observed around 150 K is assignable to the CH_3 reorientation, while the sharp one at ca. 280 K is due to the new alkyl chain motion introduced in the M_2 analysis. Around 250 K, where T_1 is approximately at a minimum, the observed M_2 shown in Fig. 1 of $(12—13)\times10^{-2}$ mT^2, which value is much larger than 7.6×10^{-2} mT^2 calculated for the model of uniaxial rotation of the whole cation about the long axis. As a possible motion with an amplitude smaller than that of the axial rotation, we propose a model of a two-site jump of the alkyl chain about its long axis by an angle 2ϕ. The M_2 calculated after the onset of this motion is given by the following equations:[20]

$$M_2(2\phi) = \frac{6}{5} I(I+1)\gamma^2\hbar^2 \Sigma R_{jk} r_{jk}^{-6}, \quad (3)$$

$$R_{jk} = [1 + 3(\sin^2\beta_{jk}\cos^2\phi + \cos^2\beta_{jk})^2]/4, \quad (4)$$

where r_{jk}, R_{jk}, and β_{jk} are the distance between the two protons, the reducing factor of M_2 and the angle between the rotation axis and the inter-proton vector, respectively. The above $M_2(2\phi)$ can be expressed as

$$M_2(2\phi) = M_2(CH_3\text{rot}) - \Delta M_2(T_1), \quad (5)$$

where $M_2(CH_3$ rot) and $\Delta M_2(T_1)$ denote the calculated M_2 for CH_3 reorientation in DACl-d_3 and the ΔM_2 derived from the T_1 minimum observed at 280 K in DACl-d_3. Substituting the calculated $M_2(CH_3$ rot) of 21.9×10^{-2} mT^2 and the observed $\Delta M_2(T_1)$ of 3.66×10^{-2} mT^2 given in Table 1 into Eq. 5, we obtained $M_2(2\phi)$ of 18.2×10^{-2} mT^2. Here, we assume the two-site jump about the cationic long axis and the tetrahedral bond angle in a DA-d_3^+ ion. Ignoring the intermolecular contribution, we obtained the jump angle between the two orientations of cation $2\phi \approx 42°$ from Eq. 3 using the obtained value of $M_2(2\phi)$.

As for DACl, T_1 values observed is LTP shown in Fig. 2 were explainable by the three superimposed minima, i.e., contributions from the CH_3 reorientation giving its minimum around 150 K, the two-site jump observed at ca. 260 K as discussed above and the NH_3^+ C_3 reorientation around 180 K expected as an additional possible motion in DACl. Using Eqs. 1 and 2, we fitted three superposed BPP-type equations to the observed data, and obtained the best fit T_1 curve shown in Fig. 2 and the motional parameters given in Table 1.

^{2}H NMR Spectra. We can also support the onset of the two-site jump of cations from the analysis of ^{2}H NMR spectra observed in LTP of DACl-d_3. Observed ^{2}H spectra on DACl-d_3 are shown in Fig. 3. Temperature dependences of the observed quadrupole coupling constant (qcc) and the asymmetry parameter η of the electric field gradient (efg) are shown in Fig. 4. The almost constant qcc value of 51 ± 2 kHz observed below 250 K is explained by the C_3 rotation of ND_3^+ group about the C–N bond axis, because, by assuming the tetrahedral bond angle, this motion reduces the qcc into 1/3 of the rigid N–D value,[21] which has been measured in $C_2H_5ND_3Cl$ as 173 kHz at 77 K.[22] With increasing temperature, the qcc began to decrease around 250 K. The fact that this temperature agrees well with those of ^{1}H M_2 and T_1 decreases shown in Figs. 1 and 2, respectively, implies that the observed ^{2}H spectrum narrowing corresponds to the two-site jump of alkyl chain as expected from ^{1}H M_2 and T_1 analyses.

When a two-site jump of the principal axis of efg at a ^{2}H nucleus by an angle of 2θ takes place, new principal components (q_x, q_y, q_z) obtainable in the rapid jumping limit can be expressed as follows, using the qcc (e^2Qq_s) and η_s values before the onset of the jump provided $2\theta < 67°35'$:[23]

$$e^2Qq_x = \frac{e^2Qq_s}{2}\left[(\eta_s - 3)\cos^2\theta + 2\right], \quad (6)$$

$$e^2Qq_y = \frac{-e^2Qq_s}{2}(\eta_s + 1), \quad (7)$$

Table 1. Motional Modes, Activation Energies (E_a), and Reductions of Second Moment (ΔM_2) Derived from ^{1}H NMR Spin-Lattice Relaxation Times T_1 and $T_{1\rho}$ Observed in $C_{12}H_{25}NH_3Cl$ (DACl) and $C_{12}H_{25}ND_3Cl$ (DACl-d_3)

Compound	E_a/kJ mol^{-1}	$\Delta M_2 \times 10^2$/mT^2	Motional mode
$C_{12}H_{25}NH_3Cl$	9.8 ± 1.0	1.38	CH_3 rotation
	13.0 ± 1.0	1.67	NH_3^+ rotation
	47 ± 2	3.66	Cationic two-site jump
	17.7 ± 1.0	—	Cationic axial rotation
	60 ± 10	—	Anionic diffusion
	100 ± 10	—	Cationic diffusion
$C_{12}H_{25}ND_3Cl$	7.8 ± 1.0	1.61	CH_3 rotation
	47 ± 2	3.66	Cationic two-site jump
	12.8 ± 1.0	—	Cationic axial rotation

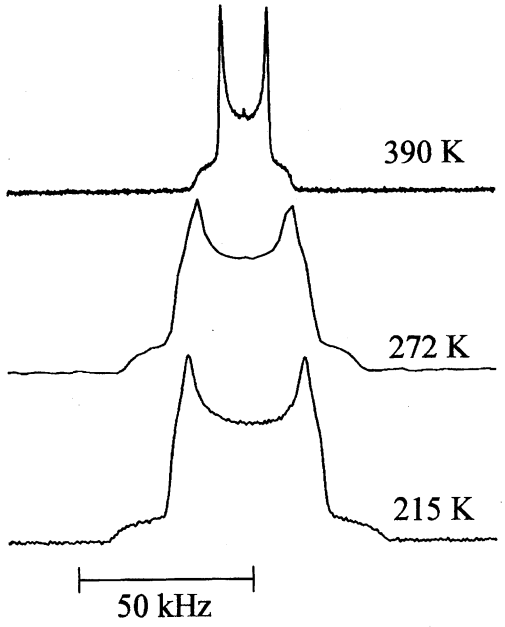

Fig. 3. ^{2}H NMR spectra observed in low-temperature phase and rotator phase of $C_{12}H_{25}ND_3Cl$ (DACl-d_3).

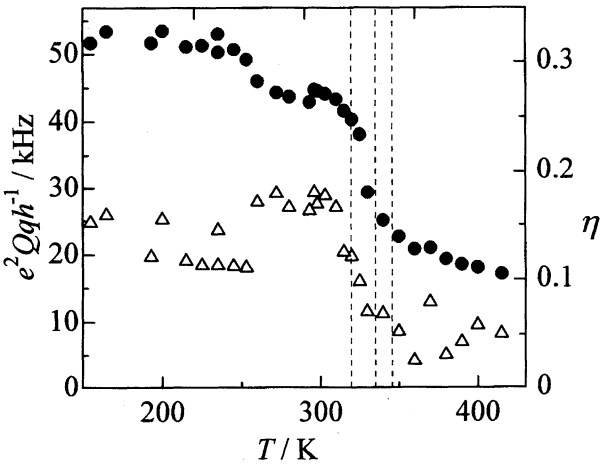

Fig. 4. Temperature dependences of ^{2}H quadrupole coupling constant (e^2Qq/h) (●) and asymmetry parameter (η) (△) in $C_{12}H_{25}ND_3Cl$ (DACl-d_3). Broken lines show the phase transition temperatures determined by DSC.

$$e^2Qq_z = \frac{e^2Qq_s}{2}\left[(\eta_s - 3)\sin^2\theta + 2\right]. \quad (8)$$

Substituting observed values of $e^2Qq_s = 51\pm2$ kHz, $\eta_s = 0.112\pm0.005$, $|e^2Qq_z| = 45\pm2$ kHz together with $\eta = 0.175\pm0.01$ observed around 270 K, where the cations are expected to perform rapid jumps, into Eqs. 6, 7, and 8, we derived $\theta = 11.1°$ giving the jump angle of the cation $2\phi \cong 39°$. This value agrees well with $2\phi = 42°$ evaluated from the ΔM_2 derived from T_1 minimum value. Choosing $\eta_s = -0.112$ as the alternative case, we obtained $2\phi \cong 89°$, which value is inconsistent with the angle derived in the ΔM_2 analysis, suggesting that the negative η_s is improbable.

The 180°-flip motion of the cation about the long axis is also an acceptable model for explaining the observed spectrum change. The possibility of this model is, however, excluded, because the calculation applying the 180°-flip results in a large value of $\eta \cong 0.8$, which is quite different from the observed $\eta = 0.175$.

Dynamics in Rotator Phase. ^{1}H NMR Second Moment (M_2). Above the three successive phase transition temperatures observed at 321, 334, and 345 K in DACl-d_3, a small M_2 value of less than 3×10^{-2} mT^2 was observed at ca. 350 K, as shown in Fig. 1. With further heating, M_2 was decreased to less than 2×10^{-2} mT^2 above 370 K. These results clearly indicate the onset of the axial rotation of cations, which has the theoretical M_2 of 7.6×10^{-2} mT^2 for DA-d_3^+ cations, as expected from the thermal and the structural analyses given above. That the observed M_2 is much smaller than the calculated value for the cationic axial rotation implies that the cationic motion is dynamically more disordered than the axial rotation. Almost the same small M_2 was observed in the rotator phases of short alkylammonium chlorides of C_4 and C_5,[3,4] indicating that nearly the same degree of disorder is attained in both the present and the short alkyl chain salts. This disorder can be attributed to the orientational distribution of the cationic long axis including effects from the conformational disorder of trans-zigzag structure of the alkyl chain. The degree of this disorder can be expressed using the order parameter S as

$$M_2(\text{obsd}) = M_2(\text{ax rot})S^2 \quad (9)$$

where M_2(obsd) and M_2(ax rot) denote the observed M_2 values and the calculated M_2 for the axial rotation of DA-d_3^+ given by 7.6×10^{-2} mT^2. The temperature dependence of evaluated S values is shown in Fig. 5. The obtained decrease in S upon heating, which indicates the averaged order for all hydrogen atoms in an alkyl chain, implies a rapid decrease of the order of alkyl chain orientation in this phase, even though the cationic centres of gravity are not completely disordered, but form a regular tetragonal lattice, as shown by X-ray diffraction.

The temperature dependence of the order parameter can be compared with those in the nematic phase reported by Saupe for typical substances,[24] which exhibited analogous decrease upon heating to that of the present system, but it is noteworthy that the order parameter in the rotator phase is almost the same or a little smaller than those in the nematic liquid crystal, indicating the high disorder even in crystalline state.

^{1}H NMR Relaxation Times (T_1 and $T_{1\rho}$). ^{1}H T_1 and the spin-lattice relaxation time in the rotating frame $T_{1\rho}$ observed in the rotator phase of DACl and DACl-d_3 are shown in Fig. 6. The almost linear increase of the log T_1 vs. T^{-1} plots observed upon heating indicates the excitation of a BPP-type motion assignable to the rapid axial rotation of cations as expected from the foregoing discussion. On the other hand, the observed $T_{1\rho}$ data could be fitted by two minima, as shown in Fig. 6, implying the onset of new motions in this phase. By referring to the $T_{1\rho}$ analysis in the rotator phases of $C_nH_{2n+1}NH_3Cl$ (n: 6—10),[5] we can assign the deep and shallow minima to the cationic and the anionic 2-D self-

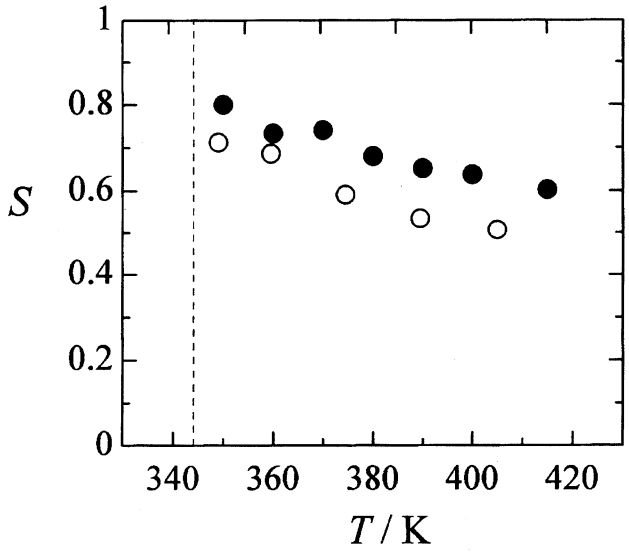

Fig. 5. Temperature dependences of the order parameters (S) derived from ^{1}H NMR second moments (M_2) (○) and ^{2}H quadrupole coupling constants (e^2Qq/h) (●) observed in the rotator phase of $C_{12}H_{25}NH_3Cl$ (DACl-d_3). Broken lines show the phase transition temperatures determined by DSC.

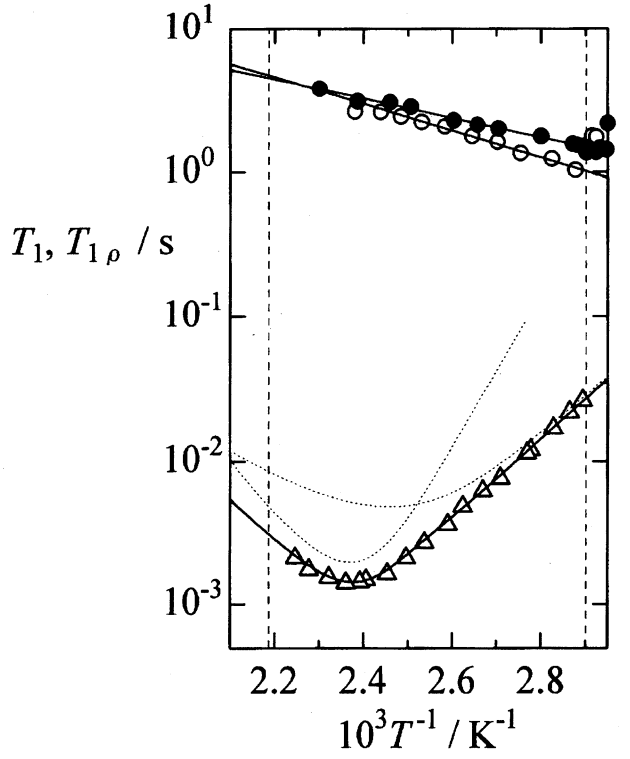

Fig. 6. ^{1}H NMR spin-lattice relaxation times T_1 (○) and $T_{1\rho}$ (△) observed in the rotator phase of $C_{12}H_{25}NH_3Cl$ (DACl) and T_1 (●) in $C_{12}H_{25}ND_3Cl$ (DACl-d_3) at Larmor frequency of 40.0 MHz and a spin-locking rf field of 0.4 mT, respectively. Solid lines are the best-fitted calculated values given in text. Dotted lines are contributions from the two relaxation mechanisms (see text). Broken lines show the phase transition temperatures determined by DSC.

diffusion, respectively. Determined activation energies are listed in Table 1. The activation energy of 100±10 kJ mol^{-1} for the cations a little larger than 70, 80, and 90 kJ mol^{-1} determined for C_8, C_9, and C_{10} analogues,[5] respectively, is explainable by the size effect of cations. On the other hand, the activation energy of 60±10 kJ mol^{-1} for the anionic diffusion comparable to 45, 40, and 50 kJ mol^{-1} obtained in C_7, C_9, and C_{10} analogues,[5] respectively, is almost independent of the chain length, supporting our assignment to the anionic motion.

The cationic diffusion is expected to take place in the 2-D layer perpendicular to the cationic long axis in the rotator phase as found in the single crystal electrical conductivity measurement on C_4 analogue.[3] It is surprising that the bulky dodecylammonium cations can perform rapid diffusional jumps in the low-temperature range just above room temperature. This result indicates that the rotator phase is a highly disordered crystalline state even in long alkyl chain salts. This nature can be compared with that in the plastic crystal in which isotropic self-diffusion as well as rotation as a whole occur with low barriers, whereas restricted motions, vs., the 2-D self-diffusion and the nearly 1-D rotation, are allowed in the rotator phase. We may, accordingly, designate the rotator phase as "a low-dimensional plastic phase" by combining these results of microscopic molecular dynamics together with the foregoing thermal data revealing the small ΔS_m less than 20 J K^{-1} mol^{-1} in contrast to the large ΔS_{tr} of 27.2 J K^{-1} mol^{-1}, which is the sum of the values at the successive three transitions to the rotator phase in DACl.

^{2}H NMR Spectra. In the present system where the layer structure contains both hydrophobic and hydrophilic groups in a cation, the degree of disorder seems to be distributed in crystals. We determined the temperature dependence of the order parameter in the NH_3^+ end in this phase from qcc values derived from ^{2}H spectra in DACl-d_3 observed above room temperature, as shown in Fig. 4. Here, we define the order parameter S as

$$e^2Qq(\text{obsd}) = e^2Qq(\text{ax rot})S, \tag{10}$$

where e^2Qq(ax rot) is the standard value (28.4 kHz) calculated for DA-d_3^+ cation axially rotating about the long axis, and the limit S=0 means the isotropic reorientation of the ND_3^+ end. This definition is acceptable, because the qcc value gives information of the asymmetry of the charge distribution around the resonant nuclei. The evaluated temperature dependence of S is shown in Fig. 5. The decrease of S upon heating indicates that the order in the polar end also decreases but a clear difference from the alkyl chain order can be seen in the figure. This indicates that the tumbling of the cationic axis is not a simple rod-like motion, but is accompanied by some conformational disorder[7] resulting in bent or kink structures of the alkyl chains.

Electrical Conductivity. We measured the electrical conductivity (σ) at 1 kHz to confirm the presence of ionic self-diffusion in the rotator phase. The temperature dependence of σT is shown in Fig. 7. Upon heating, a rapid increase

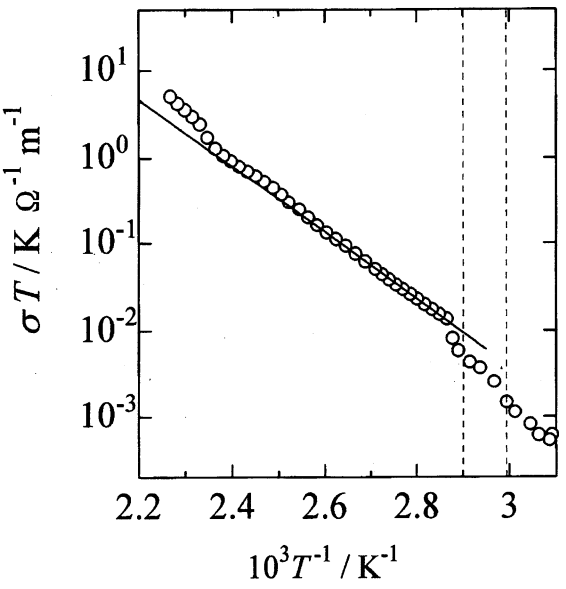

Fig. 7. A temperature dependence of electrical conductivity (σ) in the rotator phase of $C_{12}H_{25}NH_3Cl$ (DACl) measured at 1 kHz.

of σ to the order of 10^{-2} S m^{-1} was observed above 400 K, indicating the presence of ionic conduction, which supports our NMR analysis on the ionic self-diffusion. From the slope of data observed in the low-temperature range of the rotator phase shown in Fig. 7, we evaluated the activation energy of ionic diffusion to be 74 kJ mol^{-1}. This value can be assigned to the anionic self-diffusion by referring to the $T_{1\rho}$ data analysis given above. The increase of the slope at high temperatures is attributable to the onset of cationic diffusion with the high activation energy.

Conclusion

From solid NMR, X-ray powder diffraction, and thermal studies in dodecylammonium chloride, we confirmed the presence of the rotator phase between 345 and 475 K, where the bulky $C_{12}H_{25}NH_3^+$ ions perform 2-D self-diffusion as well as axial rotation about the long axis, accompanied by conformational disorder together with random tumbling of this axis. This highly disordered crystalline state having a small melting entropy less than 20 J K^{-1} mol^{-1} is quite analogous to the plastic crystals reported in molecular solids. The restricted motional freedom of cations found in the rotator phase can be compared with that in the plastic crystal in which molecular rotation and diffusion are both three-dimensional. The highly anisotropic structure in the rotator phase is also contrasted with the symmetric crystal structures such as bcc, fcc or hcp in plastic crystal. From these differences, the rotator phase can be described as "low-dimensional plastic crystal". At the same time, we note that this highly anisotropic crystalline state of lamellar-type double layer structure rather resembles the smectic liquid crystal which generally forms disordered liquid-like in-plane structure, whereas the rotator phase makes a three-dimensional regular crystalline lattice. From these results, the rotator phase can be considered as an intermediate state between the plastic crystal and the liquid crystal.

This work was partly supported by Grant-in-Aid for Scientific Research (A) Nos. 08554027 and 09440234 from Ministry Education, Science, Sports and Culture.

References

1) A. Müller, *Proc. R. Soc. London, Ser. A*, **138**, 514 (1932).
2) S. Fukada, H. Yamamoto, R. Ikeda, and D. Nakamura, *J. Chem. Soc., Faraday Trans. 1*, **83**, 3207 (1987).
3) M. Hattori, S. Fukada, D. Nakamura, and R. Ikeda, *J. Chem. Soc., Faraday Trans.*, **86**, 3777 (1990).
4) S. Iwai, R. Ikeda, and D. Nakamura, *Can. J. Chem.*, **66**, 1961 (1988).
5) S. Iwai, M. Hattori, D. Nakamura, and R. Ikeda, *J. Chem. Soc., Faraday Trans.*, **89**, 827 (1993).
6) S. B. Hendricks, *Z. Kristallogr.*, **68**, 189 (1928); R. W. G. Wyckoff, "Crystal Structures," 2nd ed, Wiley Interscience, New York (1966), Vol. 5, Chap. 14A.
7) V. Busico, P. Cernicchiaro, P. Corradini, and M. Vacatello, *J. Phys. Chem.*, **87**, 1631 (1983).
8) J. Tsau and D. F. R. Gilson, *J. Phys. Chem.*, **72**, 4082 (1968).
9) J. Timmermans, *J. Phys. Chem. Solids*, **18**, 1 (1961).
10) A. M. Levelut, *J. Phys. (France) Colloq.*, **37**, C3-51 (1976); A. J. Leadbetter, J. C. Frost, and M. A. Mazid, *J. Phys. (France) Lett.*, **40**, L-325 (1979); R. Pindak, D. E. Moncton, S. C. Davey, and J. W. Goodby, *Phys. Rev. Lett.*, **46**, 1135 (1981).
11) M. Tansho, Y. Furukawa, D. Nakamura, and R. Ikeda, *Ber. Bunsenges. Phys. Chem.*, **96**, 550 (1992).
12) M. Tansho, D. Nakamura, and R. Ikeda, *J. Chem. Soc., Faraday Trans.*, **87**, 3255 (1991).
13) H. Ishida, R. Ikeda, and D. Nakamura, *Bull. Chem. Soc. Jpn.*, **59**, 915 (1986).
14) D. C. Look and I. J. Low, *J. Chem. Phys.*, **44**, 2995 (1966).
15) J. G. Powles and J. H. Strange, *Proc. Phys. Soc.*, **82**, 6 (1963).
16) H. S. Gutowsky and G. E. Pake, *J. Chem. Phys.*, **18**, 162 (1950).
17) S. Fukada, R. Ikeda, and D. Nakamura, *Bull. Chem. Soc. Jpn.*, **57**, 2802 (1984).
18) S. Fukada, R. Ikeda, and D. Nakamura, *Z. Naturforsch. A*, **40a**, 347 (1984).
19) A. Abragam, "The Principles of Nuclear Magnetism," Oxford Univeristy Press, London (1961), Chap. VIII.
20) R. J. Pylkki, R. D. Willett, and H. W. Dodgen, *Inorg. Chem.*, **23**, 594 (1984).
21) L. W. Jeelinski, *Ann. Rev. Mater. Sci.*, **15**, 359 (1985).
22) M. J. Hunt and A. L. Mackay, *J. Magn. Reson.*, **15**, 402 (1974).
23) R. Ikeda, A. Kubo, and C. A. McDowell, *J. Phys. Chem.*, **93**, 7315 (1989).
24) A. Saupe, *Angew. Chem., Int. Ed. Engl.*, **7**, 97 (1968).